Modeling of weld bead geometry and optimization of GMAW welding parameters on CK45 steel

M. Khosravi*[1], M. Azargoman[2] , H. Torshizi[3]

Department of Mechanical Engineering, Birjand University of Technology, Birjand, Iran

Abstract

In the process of Gas Metal Arc Welding, achieving a favorable geometry meeting all requirements of the manufacturer is considered important. Therefore, for addressing these issues automated systems and modeling and optimization of the process are necessary. In the present study, empirical studies were carried out on CK45 steel considering four parameters including voltage, wire feed speed, welding speed, and welding nozzle angle as parameters affecting the welding geometry. Weld height and width were considered as the output parameter. Furthermore, for modeling the process, the surface response method was us, and finally, the process parameters were optimized using the particle pool method. The results obtained from the modeling have declared the voltage parameters of 17 wire feeding speeds of 244 welding speed of 160 and nozzle angle of 105 degrees as optimal. Examining the data predicted by the model and compared with the available experimental data, it is shown that by increasing both the wire speed and voltage and also minimizing the table speed, the width of the weld bead increases while increasing the voltage and wire speed and reducing the table speed, make the height of the bead to decrease. Hence, not only increasing the angle of the nozzle and wire-speed but also decreasing the voltage and table speed results in a decrease in the amount of dilution.

Keywords: Bead Geometry, Gas Metal Arc Welding, RSM, Optimization, Dilution.

1. Introduction

Gas Metal Arc Welding (GMAW) is defined as a multi-purpose welding process in which an electrode is constantly fed into the weld pool. An inert shielding gas such as argon is also used. The process was established in 1900 and it was industrially used in 1950 [1]. High flexibility, the possibility of welding various thicknesses, and high production rate make GMAW to be a distinct welding method [2]. Welding operations require a skillful and extensively experienced operator capable of selecting a combination of optimal welding parameters. To address the issue, many studies have been conducted to eliminate the need for a skillful operator. In order to predict the geometry of the weld bead with the capability of optimizing the welding parameters for obtaining the optimum geometry, different methods have also been introduced [3]. Due to the higher productivity, improvement of working conditions, and higher confidence level in high-quality production, automatic control systems are considered important in industrial processes. GMAW is one of the most popular welding methods [4]. This process is widely used in different industries such as gas pipeline, petro-chemistry, building, motor vehicle, and naval architecture. This process has many advantages including used electrode permanency, low discontinuity of weld, lack of slag, and low rate of thermal risk in the base metal among which the used electrode permanency is its most important advantage making the production rate increase [2]. In large industries, the production cost is of

*Corresponding author
Email:mkhosravi@birjandut.ac.ir
Address: Department of Mechanical Engineering, Birjand University of Technology, Birjand, Iran
1. Assistant Professor
2. Ph.D. Candidate
3. M.Sc

great importance and completely dependent on the determination of the welding variables. In the process of gas-shielded welding, an industrial process, there is a relationship between the existing parameters and the way of achieving ideal state, and for attaining the ideal state which is considered a costly procedure, frequent experiments are needed. Therefore, modeling based on mathematical relations is used to model the industrial systems in order to obtain an optimal point between the input and output parameters. Artificial neural networks [5] and Fuzzy logic [6] are two relevant methods, among others. Bagchi et al. [7] modeled the laser welding parameters using Taguchi method and simulated the process using three-dimensional (3D) software. They obtained an error of less than 10% compared with experiments and regression analysis. Martiner et al. [8] studied the interactions between the initial and final parameters of the GMAW process which has nonlinear behavior. In this stud,y they created a model by using image processing, despite the fact that further improvements related to image processing, computational modeling, and optimizing practical processes contribute to minimizing the initial costs. The present study has gained outstanding results for classifying the complex images and finally predicting the obtained arc parameters, pollen geometry, and penetration depth. The results of this study which aim to predict the geometry of welding pollen of GMAW process and mere compliance of this model's output data, indicate the reliability of the numerical modeling method and its obtained results, and ultimately can prove the analyses of the due time of this process. In a study, Katarav[9] optimized welding parameters to improve welding quality. In this project, in order to achieve either desirable or optimal results in design and experiments, he has examined different angles of the torch, current, wire feeding speed, and welding speed. Numerical simulations based on the finite element method for the width of the molten pool have been carried out to investigate its effect on the width and height of the weld nut. Process parameters are constructed based on using the teaching-learning optimization method in order to achieve weld pollen optimal geometry. Finally, the experiment modeling exhibits the improvement of welding quality in terms of width and height and an overall reduction in power consumption. Lee et al. [10] suggested some models predicting the weld bead based on the input parameters using the regression analysis and Taguchi method. In addition to constructing trust joints using GMAW, developing a relationship between the weld geometry and input parameters is required; as a result, for obtaining a set, the optimal parameters creating the required weld bead geometry, the interaction of variables, and the weld bead geometry should be studied. The geometry of a weld line bead plays an important role in the determination of the surface smoothness, layer thickness, and dimensional accuracy of the layered pieces. Different studies suggested that there is a significant relationship between the weld geometry and its parameters. Kolahan et al. [11] not only modeled, but also optimized the process of GMAW using a regression model and Simulated Annealing (SA) method. Evaluation of the results demonstrates the model efficiency in determining the welding parameters so that the bead geometry could be created with optimal dimensions. Multiple linear regression is an accurate modeling method considered effective in developing mathematical models of bead geometry in gas-shielded welding. Not only Back Propagation Neural Network (BPNN), but also Genetic Algorithm (GA) along with Back BPNN were applied for modeling the process. Xiong et al. [1] investigated the effect of the process parameters on the shape of weld bead components in GMAW and showed that one of the factors affecting both the weld shape and geometry is the rate of the arc current. The process parameters were all selected based on the experiments or extracted from the databases. It should be noted that input parameters chosen by this method may not produce the required weld bead; therefore, producing models providing the relationship between the geometry of weld bead and the process variables sounds is necessary. In the present research, wire-speed(WS), table speed (TS), voltage (V), and welding nozzle angle (NA) were considered as the effective input parameters of the process and, according to the research requirements, weld bead height (R), bead width (W), penetration depth (P), the surface above weld the (A), the surface below weld (B), and dilution percent (D) were output parameters. The response surface method (RSM) was used to establish a relationship between the output and input parameters of the process. The present study aims to model the output parameters based on the inputparameters and also to optimize the dilution percent.Finally, the joint which was produced using the optimized parameters was investigatedto evaluate the microstructure and the mechanical properties.

2. Experiments

Gas Metal Arc Welding has a wide range of applications. In this method, the temperature resulted from the arc created between a continuous feeding wire and work piece along with the support of a neutral gas such as Helium or Argon or an active gas such as carbon dioxide or a mixture of these gases create the weld pool and then the welding is performed [12]. The welding process is shown schematically in Figures 1 and 2.

The experiments were conducted using Cthe arry MIG 501 welding machine and Pars Feed 4520 C feeding system of wire.

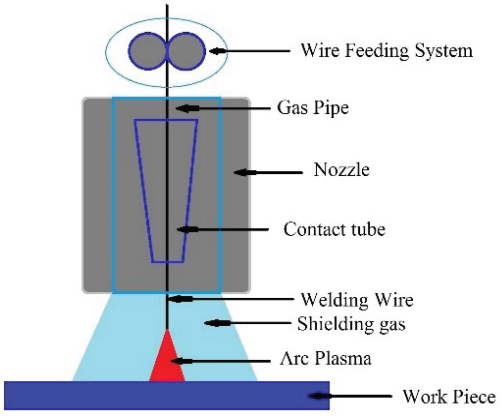

Fig. 1 Schematic of gas metal arc welding.

Fig. 2 Gas metal arc welding set-up.

2.1. The base metal and electrode

Achieving conditions for obtaining the maximum mechanical properties along with maintaining the simplicity of the heat treating system and its cost-effectiveness is of great importance. Thus, in the present study, CK45 steel pieces with dimensions of 10×30×50 mm were used as the base metal in GMAW. The chemical composition and mechanical properties of CK45 are shown in Tables 1 and 2, respectively.

The AMA 40-18 M electrode was used according to the DIN 8559 SG2 with a diameter of 1.2 mm, see Table 3 for the chemical composition.

2.2. Experiment design

Since many studies have been performed on the parametric study of the arc welding process with shielding gas [13]. In the research, the supply speed of the wire (electrode) was performed, voltage, welding speed, and Nozzle Angle was considered was effective input parameters. The parameters were examined at three levels and the total number of experiments was 81. To measure the wire feeding speed, the length of the output wire from the nozzle opening was measured at a certain time. Then the output speed in centimeters per minute was obtained. IToprecisely adjusts the welding speed, in this research, FP4M Milliann ng table and four of our-movement twere used. Parameter levels are shown in Table 4.

Table 1. Chemical composition of CK45 (DIN 17200) steel.

C (%)	Si (%)	Mn (%)	P (%)	S (%)
0.42–0.50	0.15–0.35	0.15–0.35	0.035	0.35

Table 2. Mechanical properties of CK45 (DIN 17200) steel.

бr (MPa)	бc (MPa)	εr (%)	Hardness HB
670–820	420	>16	205

Table 3. Chemical composition of Consumable electrode.

C	Si	Mn	P	S	Fe
0.06-0.12	0.7-1	1.3-1.6	≤0.025	≤0.025	Bal

Table 4. GMAW Parameters.

No	interval	Unit	Input Parameters
1	17-27	V	Voltage
2	207-244	cm\min	Wire Speed
3	160-250	mm\min	Table Speed
4	75-105	°	Nozzle Angle

In this study, as shown in figure 3, the output parameters included weld bead height (R), weld bead width (W), penetration depth (P), upper weld surface (a), lower weld surface (b), and dilution ratio percentage consisting of the dilution rote percentage of the filler metal with the base metal computed using both upper and lower surface of the weld according to Equation 1.

$$\%Dilution = [\frac{b}{A+B}] \times 100(1) \qquad \text{Eq.(1)}$$

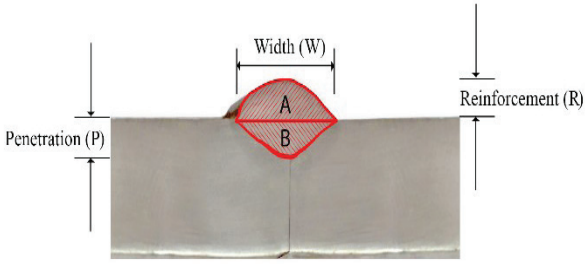

Fig. 3. Cross-section of the weld bead.

2.3. Cross-section evaluation

To diagnosis the weld cross-section and measure the output parameters, the joints were cross-sectioned, etched using diluted nitric acid (see figure 3). The machine vision and image processing techniques were used for measuring the output parameters. For imaging, a DFK-23GM021 camera with a data collecting rate of 60 frames per second and a resolution of 1280×960 and a CCD sensor were used. An ML614-MP2 lens with a diameter of 30 mm and a focal distance of 12 mm was applied.

2.4. Image processing

MATLAB R2016b software was used for image processing. Before processing, the calibration was performed to eliminate the vision error. Indeed, factors including position vector and origin spin matrix of the camera were compared to the general origin of coordinates which was the same coordinate system on the images that were measured. In the case of a fixed camera, calibration was only done once. The calibration images were included one with circular points of the same size with a diameter of 10 mm, as shown in figure 4. The plane images were captured in different conditions and an image processing software was calibrated in each condition. To ensure the accuracy of the calibration and machine vision system, a block gage withe the length of 10 mm and an accuracy of 0.001 mm was used according to figure 4. The results of this validity check are shown in table 5.

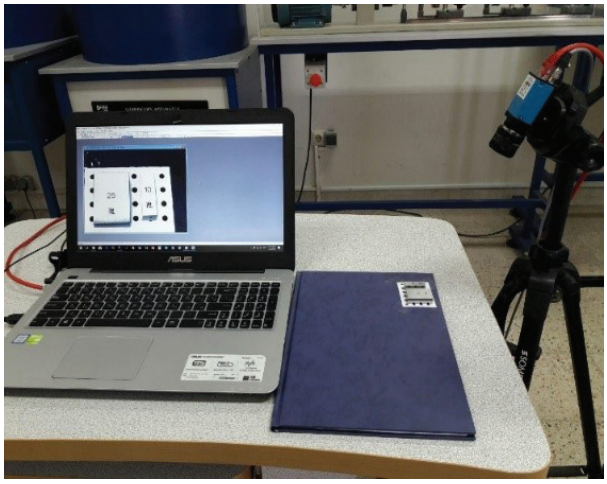

Fig. 4 The block gage for validity check.

Table 5. The block gage measuring results.

	Accuracy mm	Nominal mm	Measuring mm	Error mm
Block Gage	0.001	10	9.93	0.07

These experiments were performed and output parameters such as weld bead width (w), weld bead height (R), penetration depth (P), upper weld surface (A), lower weld surface (B), and dilution percentage were obtained using image processing are shown in Table 6.

3. Tensile test

The standard tensile test was performed in order to investigate the mechtoerties of the optimized piece. In this experiment, the test piece was prepared according to ASTM–E8. The tensile specimen is shown in figure 5. The Zwick/Roell Z600 machine was used to perform the tensile test. The result of the tensile test is shown in figure 6.

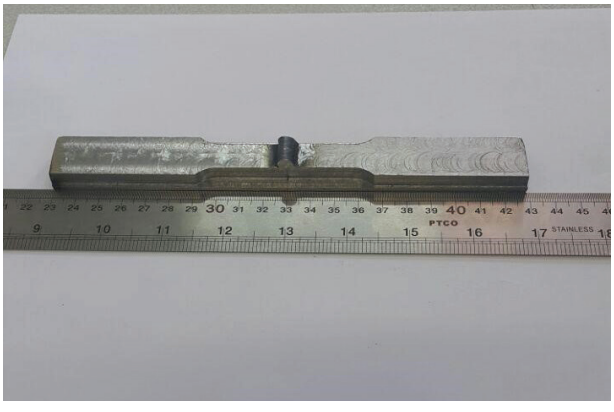

Fig. 5.Tensile test specimen.

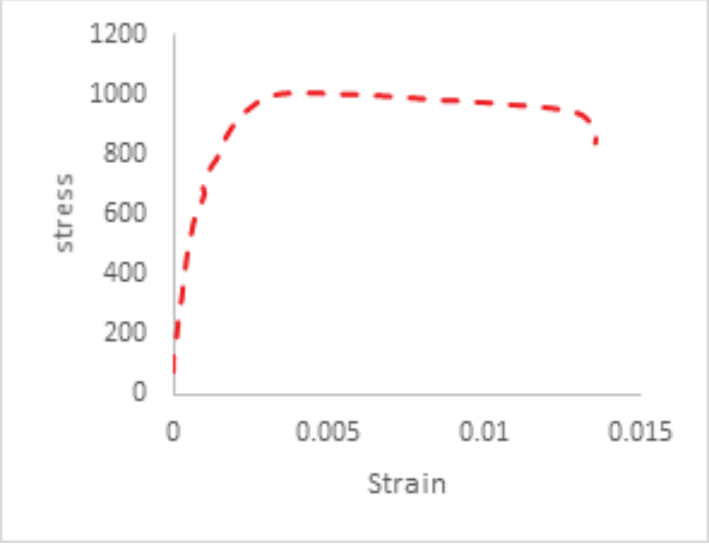

Fig. 6.Stress-strain curve for optimized specimen.

4. Developing a model using the response surface method

In the response surface method, the interaction between several descriptive variables and one or more response variables is investigated. Response surface method is a strategy for constructing and optimizing an empirical model. In the current research, using the regression analysis, a model of the relation of the response to several independent input varibles, was obtained.

In the response surface method, independent parameters can be indicated based on Equation 2.

$$y = f[x_1.x_2.x_3 \dots x_n] \quad \text{Eq.(2)}$$

Where y is the response, f is the response function, y is the experimental error, x_2 x_n are independent parameters.

Developing the expected response y, a surface known as response surface is obtained. The shape of the function f is unknown and maybe more complicated. Therefore, the response surface method aims to approximate f with a polynomial of a lower order in relation to several independent variables of the process. If the response is properly modeled by a linear function of the independent variables, Equation 2 can be written as [13].

$$y = \beta_0\beta_1 x_1 + \beta_2 x_2 + \beta_3 x_3 + \cdots + \beta_n x_n \quad \text{Eq.(3)}$$

Nonetheless, if a curve appears in the system, we can use a polynomial of the higher-order) as follows [14].

$$y = \beta_0 + \sum_{i=1}^{k} \beta_i x_i + \sum\sum_{i<j} \beta_{ij} x_i x_j + \sum_{i=1}^{k} \beta_{ii} x_{i^2} + \varepsilon \quad \text{Eq.(4)}$$

When a dependent data set is collected using an empirical experiment set, an appropriate statistical analysis such as ANOVA analysis is carried out to determine the effects of the independent factors on the dependent outputs and also interactions between the factors [15]. Then, the improved model is confirmed by a verification test. In this paper, MINITAB 18 software has been used for modeling.

5. Results and Discussion

The developed model using MINITAB is investigated in this section. The obtained relations to model and predict the welding process outputs are shown in Equations 5, 6, 7, and 8.

Weld Bead Width =, 9.07 + 1.2 V- 0.59 SW – 1. 01V2 Eq.(5)

Weld Bead Height = 2.34 -0.605V +0.571 SW +0.435 V2 Eq.(6)

Penetration Depth = -86.1 +0.634V + 0.707 SW - 0.02 V2 Eq.(7)

Dilution = 52.86 + 7.45 V – 4.42 SW -10.9 V2 Eq.(8)

In the above relations, V is voltage and SW is wire speed. To confirm the accuracy of the relations, variance analysis was used. The confidence level of the obtained model is 95% when the P-value is less than o.o5.Tables 7, 8, 9 and, 10 indicate the results of the variance analysis.

Table 6. Results of experiments.

No.	V (v)	SW (cm/min)	ST (mm/min)	AN (deg.)	P (mm)	R (mm)	W (mm)	A (mm^2)	B (mm^2)	D (%)
1	17	207	160	90	1.789	3.26	5.643	12.124	6.482	34.838
2	22	207	160	90	1.806	2.011	8.881	2.017	9.828	82.971
3	27	207	160	90	2.398	2.375	11.261	15.743	14.458	47.872
4	17	215	160	90	1.602	1.331	8.025	7.502	8.413	52.862
5	22	215	160	90	3.484	2.444	9.407	15.571	15.423	49.741
6	27	215	160	90	3.657	2.545	13.206	24.259	26.515	52.221
7	17	244	160	90	1.575	4.58	7.47	27.643	5.197	15.825
8	22	244	160	90	2.678	1.37	10.224	9.916	14.799	59.878
9	27	244	160	90	2.125	2.93	8.065	17.641	8.621	32.826
10	17	207	200	90	1.47	1.934	11.195	16.206	20.288	55.592
11	22	207	200	90	3.202	1.647	8.56	9.363	15.966	63.034
12	27	207	200	90	3.697	1.058	9.852	8.043	21.968	73.199
13	17	215	200	90	1.07	4.858	9.049	34.933	2.521	6.73
14	22	215	200	90	4.33	2.305	7.87	14.525	18.24	55.669
15	27	215	200	90	1.98	2.519	5.167	9.483	7.683	44.757
16	17	244	200	90	2.38	4.654	6.445	21.848	14.525	39.933
17	22	244	200	90	3.926	2.819	8.828	17.046	20.408	54.488
18	27	244	200	90	3.865	2.516	11.635	20.288	22.208	52.259
19	17	207	250	90	1.543	1.655	6.867	8.425	6.95	45.203
20	22	207	250	90	1.882	1.403	6.068	5.425	7.605	58.365
21	27	207	250	90	1.842	1.699	8.926	9.695	11.326	53.879
22	17	215	250	90	1.843	2.88	5.05	9.62	11.016	53.382
23	22	215	250	90	2.34	2.191	7.911	11.048	9.941	47.362
24	27	215	250	90	3.503	1.556	9.885	9.744	21.033	68.339
25	17	244	250	90	1.557	2.562	5.873	9.786	7.262	42.597
26	22	244	250	90	2.962	1.564	8.901	10.88	14.417	56.99
27	27	244	250	90	1.384	4.126	7.024	25.159	4.903	16.309
28	17	207	160	75	1.696	2.898	4.51	10.914	5.674	34.205
29	22	207	160	75	1.964	2.72	9.152	19.241	11.596	37.604
30	27	207	160	75	2.284	1.776	6.52	7.784	7.812	50.089
31	17	215	160	75	3.33	2.642	9.498	19.013	18.289	49.029
32	22	215	160	75	3.406	2.874	8.856	18.03	15.072	45.531
33	27	215	160	75	3.158	2.953	9.24	19.679	16.386	45.434
34	17	244	160	75	1.008	5.695	4.146	24.509	2.328	26.185
35	22	244	160	75	3.572	4.109	10.262	31.432	18.119	69.011
36	27	244	160	75	2.489	1.875	9.471	12.542	14.665	8.674
37	17	207	200	75	1.292	2.852	5.005	10.537	3.738	36.566
38	22	207	200	75	2.089	1.313	7.396	6.533	14.549	60.319
39	27	207	200	75	1.623	1.78	9.418	11.192	17.013	53.901
40	17	215	200	75	2.303	3.338	5.154	14.605	7.92	35.16
41	22	215	200	75	2.97	1.912	9.698	12.045	20.92	63.461
42	27	215	200	75	2.611	1.626	9.454	11.488	15.926	58.094
43	17	244	200	75	3.102	2	12.045	17.844	19.081	51.675
44	22	244	200	75	3.337	2.062	11.91	16.862	20.641	55.038

45	27	244	200	75	2.97	2.84	12.071	22.458	19.221	46.116
46	17	207	250	75	1.984	2.509	4.506	6.995	4.334	38.255
47	22	207	250	75	2.032	2.153	6.347	8.337	7.72	48.078
48	27	207	250	75	1.816	1.789	8.404	9.967	8.996	47.439
49	17	215	250	75	1.447	3.943	3.602	10.679	3.913	26.816
50	22	215	250	75	2.769	3.045	8.324	20.707	13.492	39.451
51	27	215	250	75	3.25	1.875	8.833	9.472	15.528	62.112
52	17	244	250	75	0.918	6.012	2.698	15.447	1.779	10.327
53	22	244	250	75	4.915	1.932	12.875	18.691	31.461	62.731
54	27	244	250	75	3.375	2.279	8.513	11.875	15.037	55.874
55	17	207	160	105	1.003	3.193	6.49	15.95	7.12	30.862
56	22	207	160	105	3.76	2.757	8.699	16.263	14.745	47.552
57	27	207	160	105	2.525	1.387	9.431	9.211	13.869	60.09
58	17	215	160	105	2.537	3.555	6.742	20.429	7.704	27.384
59	22	215	160	105	3.19	1.236	10.316	10.781	15.062	58.282
60	27	215	160	105	1.354	1.984	7.598	11.753	6.55	35.786
61	17	244	160	105	0.954	5.654	9.567	48.184	2	3.985
62	22	244	160	105	2.27	3.894	10.826	32.445	11.895	26.826
63	27	244	160	105	4.839	2.128	13.183	20.958	30.974	59.643
64	17	207	200	105	1.704	2.402	6.618	12.233	5.189	29.784
65	22	207	200	105	1.678	1.785	6.791	8.527	7.646	47.276
66	27	207	200	105	2.201	2.275	9.508	13.719	13.58	49.745
67	17	215	200	105	1.759	3.286	7.18	18.092	5.764	24.161
68	22	215	200	105	2.783	2.459	9.445	15.79	11.94	43.058
69	27	215	200	105	1.847	3.337	4.293	13.328	5.584	29.526
70	17	244	200	105	2.59	4.14	6.756	21.711	8.92	29.12
71	22	244	200	105	2.506	3.884	9.278	29.007	12.701	30.452
72	27	244	200	105	3.696	2.418	11.856	19.322	22.072	53.321
73	17	207	250	105	2.99	2.101	10.613	14.378	17.521	54.926
74	22	207	250	105	2.937	2.129	10.192	14.154	18.092	56.106
75	27	207	250	105	1.55	1.036	7.543	5.214	7.428	58.756
76	17	215	250	105	2.773	4.264	9.333	29.397	15.488	34.505
77	22	215	250	105	2.495	2.04	7.822	11.623	9.35	44.581
78	27	215	250	105	2.722	1.37	8.898	7.823	14.196	64.741
79	17	244	250	105	2.904	3.062	5.12	9.668	6.956	41.843
80	22	244	250	105	1.87	3.11	10.242	8.252	14.212	63.265
81	27	244	250	105	3.377	2.52	11.139	18.052	20.229	52.843

Table 7. Variance analysis for weld bead width model.

Source	DF	Adj SS	Adj MS	F-Value	P-Value
Model	3	116.08	38.069	9.45	0.000
Linear	2	97.7	48.85	11.93	0.000
V	1	78.71	78.7	19.22	0.000
SW	1	18.99	18.99	4.64	0.034
Square	1	18.381	18.381	4.79	0.037
V2	1	18.381	18.381	4.79	0.037
Error	77	315.31	4.095		
Total	80	431.391			

Table 8. Variance analysis for weld bead height model.

Source	DF	Adj SS	Adj MS	F-Value	P-Value
Model	3	40.8	13.6	20.01	0.000
Linear	2	37.39	18.69	27.51	0.000
V	1	19.787	19.7871	29.11	0.000
SW	1	17.61	17.61	25.91	0.000
Square	1	3.408	3.4078	5.01	0.028
V*V	1	3.408	3.4078	5.01	0.028
Error	77	52.33	0.6797		
Total	80	93.142			

Table 9. Variance analysis for weld bead penetration depth model.

Source	DF	Adj SS	Adj MS	F-Value	P-Value
Model	3	19.1	6.36	10.58	0.000
Linear	2	13.151	6.57	10.92	0.000
V	1	8.178	8.178	13.59	0.000
SW	1	4.973	4.9728	8.26	0.005
Square	1	5.649	5.949	9.88	0.002
V*V	1	5.949	5.9493	9.88	0.002
Error	77	46.35	0.602		
Total	80	65.452			

Table 10. Variance analysis for dilution model.

Source	DF	Adj SS	Adj MS	F-Value	P-Value
Model	3	8186	2062	11.76	0.000
Linear	2	4047	2023.6	11.54	0.000
V	1	2994	2994	17.08	0.000
SW	1	1053	1053	6.01	0.017
Square	1	2139	2139	12.2	0.001
V2	1	2139	2139	12.2	0.001
Error	77	13500	175.3		
Total	80	19686			

P-Value less than five percent in Tables 9 and 10 shows a good fit between the mode parameters in the process, and due to the appropriateness of the equations, the interaction of the input and output parameters is reported separately here. Figure 5 shows the response level for wire speed and voltage with respect to the width of the weld nut. Increasing the voltage and speed of the wire increases the width of the weld nut.

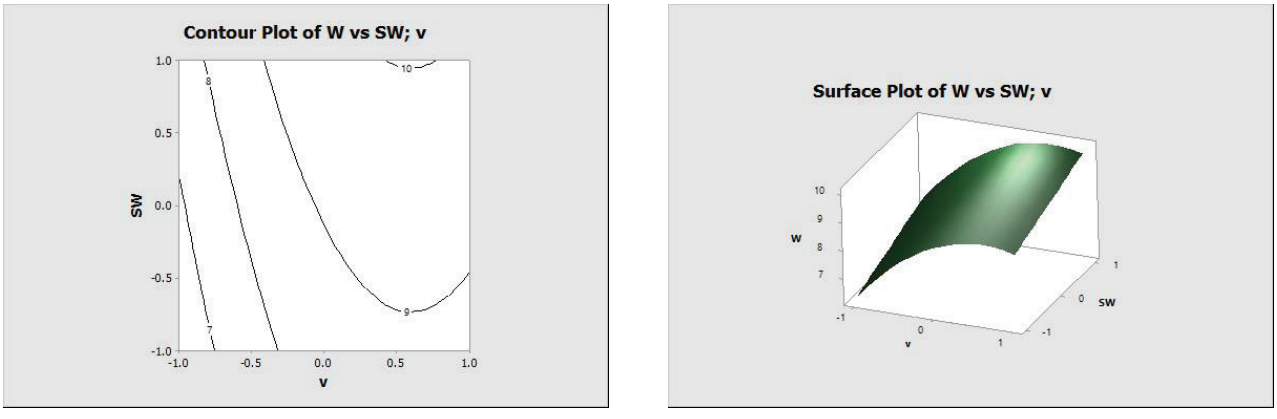

Fig. 7. Interaction of wire speed and voltage across the welded bead width.

Figure 8 indicates the interaction of voltage and wire speed regarding the weld bead height. This figure suggests that increasing the voltage and also decreasing the wire speed makes the weld bead height increase.

Better grain growth and the creation of an optimal joint require a higher depth of weld penetration in the base metal. Figure 9 the interaction of the wire speed and voltage with the penetration depth. To maximize penetration depth, the welding speed should be increased and the voltage should be moderated.

Figure 8 presents the interaction of the wire speed and voltage regarding; dilution percent. This figure suggests that any increase in the wire speed and voltage reduces the dilution.

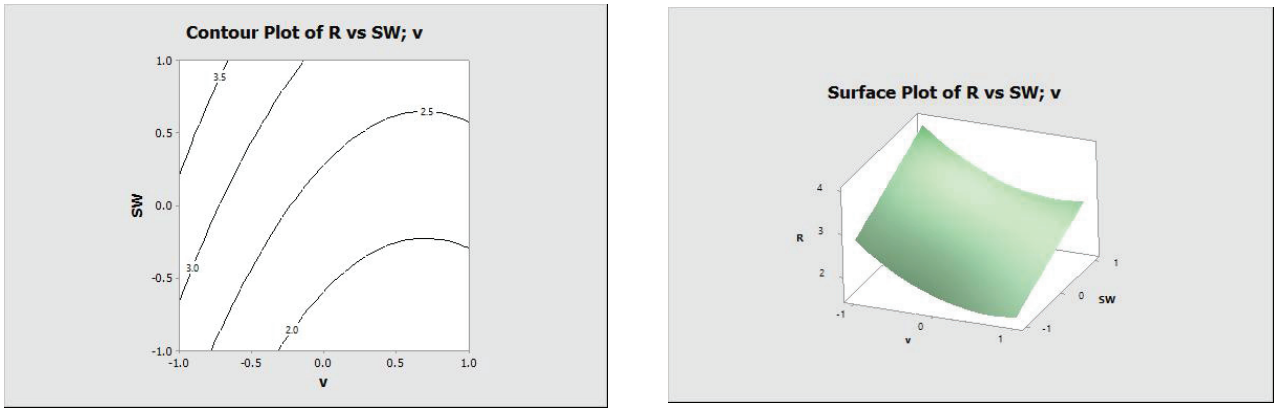

Fig. 8. Interaction of the voltage and wire speed regarding the height of the weld bead.

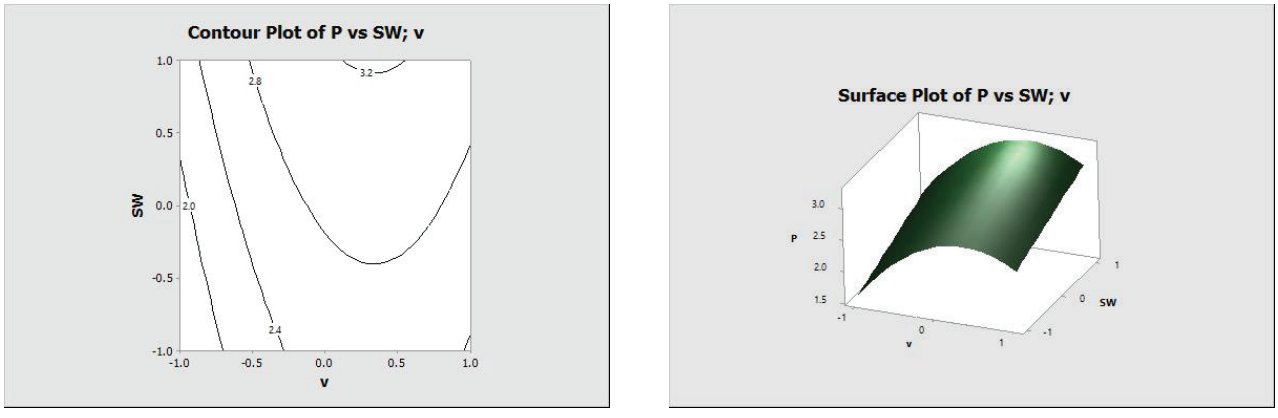

Fig. 9. Interaction between the voltage and wire speed regarding the penetration depth.

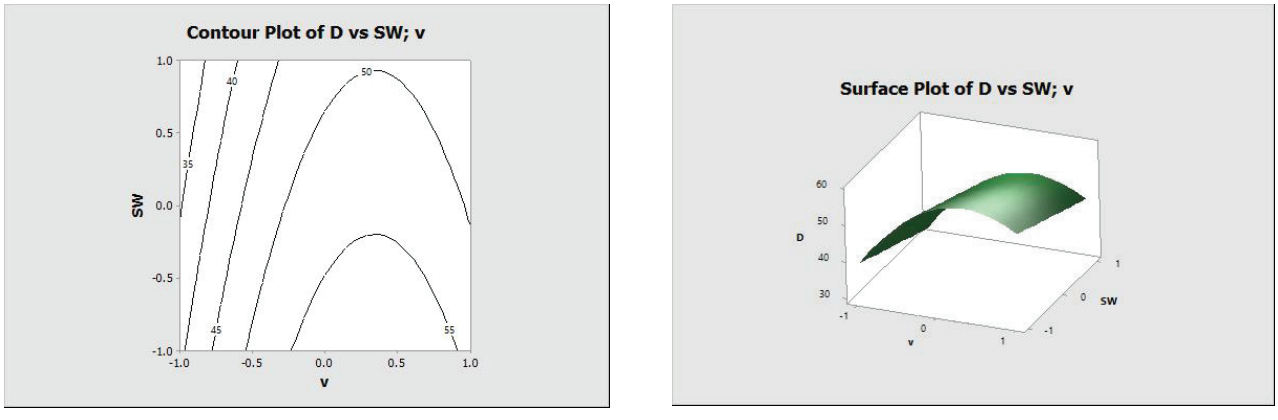

Fig. 10. Interaction of the wire speed and voltage regarding the dilution.

In this research, in addition to modeling the output parameters, the voltage (V), wire-speed (WS), table speed (TS), and nozzle angle (NA) were optimized to minimize the dilution percentage using both MINITAB software and the response surface method. Figure 9 According to studies conducted during the arc welding process, all efforts are made to create a pollen geometry that has all the desired parameters. An attempt has been made to introduce a sample. Shows the optimization performed using the mini tab. The variables of voltage, wire feeding speed, welding speed, and welding angle with the numbers 17, 244, 160, and 105 degrees, respectively, have created the optimal sample and presented the desired results. But to achieve the desired results, experiments were performed with 81 samples.

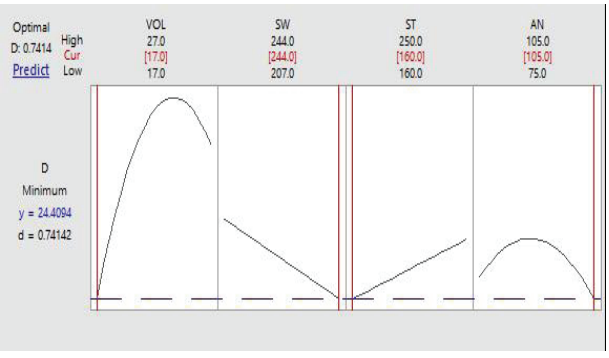

Fig. 11. Results of the optimization using the response surface method.

To check the validity of the optimization, an empirical test was performed using optimal values and its result is presented in figure 12. Table 11 shows the optimal values of both dilution accuracy check test and error percent. As shown in Table 11, the error rate is less than 0.1 percent and this suggests that the optimization is acceptable.

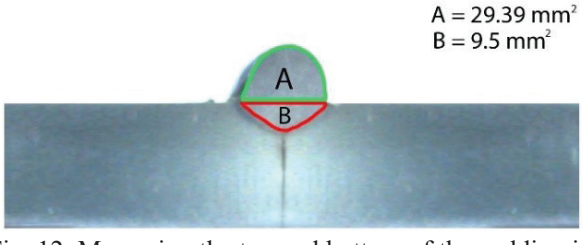

Fig. 12. Measuring the top and bottom of the welding in the optimized joint.

Metallography and tensile test were also performed on the optimized test pieces which are discussed here. In this section, microstructural changes of the weld metal and the heat-affected zone regarding the changes of wire feeding speed, welding speed, and voltage are investigated. The main role of shielding gas is protecting the melted metal against nitrogen and oxygen, existing in the atmosphere, and the creation of a whole. In this process, carbon monoxide gas is considered as insulation and creates a welding arc. The arc created at a high temperature prevents oxygen from entering and reacting in the welding area. Because the entry of any material from the atmosphere in the welding area increases the structural defects and has a negative effect in this area. This is why there is a limited number of inclusions in this method. Carbon dioxide also increases the volume fraction of the Widmanstatten ferrite and the melt penetration depth. Due to the good electrical conductance of copper, Copper-coated filler metal was used here for improving electric arc and facilitating smooth movement of the wire. Considering figure 13-b, and that the fact that the heat reduction in the welding area is one of the advantages of the arc welding method with shielding gas. The low heat generated accelerates the refrigeration in the welding area and causes that the microstructures include the phases of polygonal ferrite (PF), Widmanstatten ferrite (WF), and acicular ferrite (AF). The black points are holes and inclusions. According to the prototype and increase the refrigeration speed Welding decreased the size of grains and the Widmanstatten ferrite fraction and increased the acicular ferrite fraction. The separating line of the weld metal and the weld zone is slight and the heat-affected zone is well defined. In the weld pool, the column and interwoven growth of Widmanstatten ferrite are observed getting small and stopping in the melt zone, and in this zone, we find the presence of polygonal ferrite and acicular ferrite. As shown in figure 13-a, the heat-affected zone, nearby the base metal, contains more grain boundaries and smaller grains compared with the base metal resulting in mechanical properties improvement. Contrary to the zone near the weld metal, this zone shown in figure 13-b has a finer structure as a result of its rapid cooling.

Increasing the gap between the welding nozzle and the workpiece has a positive effect on reducing the amount of heat transfer and temperature stored in the welding area and, accordingly, reduces the grain growth time. As was

Table 11. Comparing validation and optimized.

Results		
Error percentage	Dilution in the validation test	Optimized dilution
0.073	24.427	24.409

shown, in the zone of slight melting adjacent to the weld metal, acicular ferrite was formed but the same structure of the base metal, namely polygonal ferrite, and a little perlite were found in the heat-affected zone.

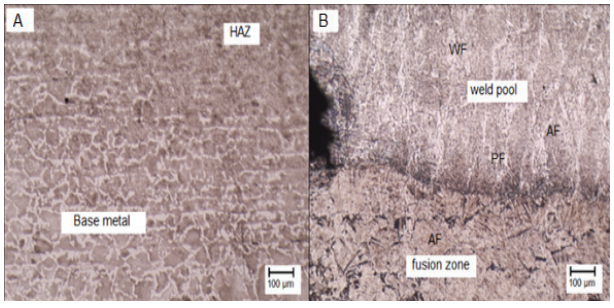

Fig. 13. (a) Microstructure of the base metal and heat affected zone (b) microstructure of welding and minor melting area, etched in 2% nital X100 magnification.

6. Conclusion

- Considering the P-value in the variance analysis tables of outputs, It can be concluded that the model developed using the response surface method is considered reliable.
- To achieve the best value and increase the width of the welding geometry, to create more heat, the voltage variable should be at the maximum and the welding speed should be at the lowest size, the nozzle angle is vertical and the electrode feeding speed in the conditions Be placed in the middle.
- To reduce the height of the pollen geometry created by welding, applying the maximum amount of voltage variable to increase the welding depth and reduce the feeding rate of the electrode is the main determinant..
- To increase the penetration depth, according to the relationship between the two variables of voltage and welding speed and the direct effect of these two variables on each other, the average values in the variable of voltage and welding speed can be adjusted.
- Due to the fact that the right amount of dilution is required to create a weld with pollen geometry, the variable of electrode velocity at maximum and voltage at minimum is possible.
- The reliability of the response surface optimization was validated using a validation test.

Reference

[1] J. Xiong, G. Zhang, J. Hu, L. Wu: J. of Int. Manu., 25(2014), 57.

[2] M. Anzehaee, M. Haeri: J. of Proc. Con., 22(2012), 1087.

[3] A. Siddaiah, B. K. Singh, P. Mastanaiah: Int. J. of Adv. Manu., 89(2017), 27.

[4] D. Yang, C. He, G. Zhang: J. of Mat. Proc. Tech., 227(2016), 153.

[5] T. Khanna: Foundations of Neural Networks, Addison Wesley, New York, (1990).

[6] S. Cammarata: Sistemi a Logica Fuzzy, Etaslibri, Italia(1997).

[7] A. Bagchi, S. Saravanan, G. S. Kumar, G. Murugan, K. Raghukandan: Opt., 146(2017), 80.

[8] R. T. Martínez, G. A. Bestard, A. M. A. Silva, S. C. A. Alfaro: J. of Manu. Proc., 62(2021), 695.

[9] K. Venkatarao: J. of Clea. Prod., 279(2021), 123891.

[10] W. Lee, C. Wei, S. Chung: J. of Mat. Proc. Tech., 214(2014), 2366.

[11] F. Kolahan, M. Hydari: Int. J. of Mec. Sys. Sci. Eng., 2(2010), 138.

[12] N. SV: Modern ARC Welding Technology, Oxford and IBH, New Delhi, (1988).

[13] Z. Liu, D. Zhao, P. Wang, M. Yan, C. Yang, Z. Chen, J. Lu, Z. Lu: J. of Mat. Sci. and Tech., 100 (2022), 224.

[14] M. Gangil, M. K. Pradhan: Mat. Tod. Proc., 4(2017), 1752.

[15] M. A. Bezerra, R. E. Santelli, E. P. Oliveira, L. S. Villar, L. A. Escaleira: Tala., 76(2008), 965.

[16] M. Mia: Meas., 121(2018), 249.